Fracture properties of an irradiated PWR UO2 fuel evaluated by micro-cantilever bending tests

Ronan Henry, Isabelle Zacharie-Aubrun, Thierry Blay, Smail Chalal, Jean-Marie Gatt, Cyril Langlois, Sylvain Meille

Fracture properties of an irradiated PWR UO_2 fuel evaluated by micro-cantilever bending tests

Ronan Henry [a,b], Isabelle Zacharie-Aubrun *[b], Thierry Blay [b], Smail Chalal [c], Jean-Marie Gatt [b], Cyril Langlois [a], Sylvain Meille [a]

[a] *Université de Lyon, INSA Lyon, MATEIS UMR CNRS 5510, 7 avenue Jean Capelle, 69621 Villeurbanne, France*

[b] *CEA, DEN, DEC, Cadarache, 13108 Saint-Paul-Lez Durance, France*

[c] *Carl Zeiss S.A.S, Division Microscopie et Systèmes, 100, route de Versailles, 78161 Marly le Roi, France*

** Corresponding author: isabelle.aubrun@cea.fr*

Keywords

Micro-cantilever bending test; Fracture properties; Focused ion beam; Irradiated UO_2 fuel; Grain boundaries; Crystallographic planes

Highlights

- Micro-cantilever bending method was applied to an irradiated PWR UO_2 fuel for the first time.
- Micro-cantilever specimens were prepared by FIB. Bending tests were then conducted with a nano-indenter up to failure.
- Fracture parameters (local strength and local toughness) of an irradiated PWR UO_2 fuel were evaluated.
- A comparison of fracture strength was made between different microstructural features: crystalline planes of single grains and grain boundaries.

Abstract

For the first time, fracture properties of a UO_2 fuel preliminary irradiated in a Pressurized Water Reactor (PWR) were characterized by bending tests. Measurements were made at room temperature and at a local scale on micro-cantilevers. Notched and un-notched specimens were prepared with a Focalized Ion Beam (FIB) microscope. Some cantilevers were milled into single grains of the polycrystalline UO_2 fuel sample with specific crystallographic orientations chosen with Electron BackScatter Diffraction (EBSD) measurements, others were milled in order to test grain boundaries. Then, every specimen was tested up to failure with a nano-indenter *in situ* of the SEM/FIB chamber. The resulting brittle fracture parameters (fracture toughness and fracture stress) are compared and discussed. Grain boundaries exhibit a significantly lower fracture resistance than grains, and {111} crystallographic planes appear weaker than {100} and {110} planes in single grains.

1. Introduction

The nuclear UO_2 fuel of Pressurized Water Reactor (PWR) is a refractory ceramic sintered into pellets. During service, the heat produced by the nuclear reaction is transferred to the coolant by thermal conduction, leading to a significant difference of temperature between the pellet center, at a temperature of around 1000°C, and the pellet periphery, at a temperature of around 500°C. At the first power rise, this gradient generates systematically large cracks which divide pellets into a few pieces. Moreover, during power transients, additional cracking is generated at the pellet periphery [1], and for simulated accidental situations, the rise of temperature leads to a complete fracturing of the fuel [2] or to an extensive cracking of grain boundaries in the periphery of the fuel pellet [3]. To

model numerically the fuel brittle cracking in PWRs in each of these situations, it is necessary to measure the fuel fracture properties and their evolution with irradiation. The two main parameters needed are the fracture toughness K_{IC} and the fracture stress σ_R [4]. Both have already been measured on fresh fuel with conventional macroscopic methods [5][6], however it is impossible to machine macroscopic specimens on irradiated fuel because of pellet cracking.

In a preliminary work, the micro-cantilever method has been set up and validated on a model material of the nuclear fuel, the cubic zirconia [7]. It allows the determination of a local fracture stress and a local fracture toughness of different crystalline planes in single grains of the material. Micro-cantilever tests are known to be very useful to probe the fracture properties of small samples, however the results of such tests should be taken only as an estimation of fracture properties [8]. The fracture stress suffers from an important scale effect and leads to high values of typically several GPa for micron-size specimens. The proposed reason is generally linked to the size of flaws inducing the fracture [9], much smaller in micro-specimens than in macroscopic samples. For fracture toughness measurement, it has been shown that the micro-mechanics approach works well on brittle materials [10]. However, because of the larger fracture process zone on semi-brittle and ductile materials, further precautions have to be taken [11].

The goal of the present work is to use the micro-cantilever bending method to study the fracture behavior of irradiated PWR UO_2 fuel. Micro-cantilever tests have already been carried out on fresh nuclear fuel [12] or on irradiated materials [13], but to our knowledge, never on irradiated fuels. Different features of the irradiated fuel microstructure are probed: crystalline planes of single grains and grain boundaries.

2. Experimental details

2.1. Materials

The sample was prepared in a UO_2 fuel with an average grain size of around 60 µm, such large grains being obtained by the addition of chromia Cr_2O_3 before pressing and sintering. The fuel was irradiated in a PWR at the sample average burn-up of 35.4 GWd/tU, while the tested area in the center of the pellet underwent a local burn-up of 34.1 GWd/tU. The examination of the irradiated fuel was conducted in the hot cells of the CEA LECA-STAR facility at Cadarache (France).

The fuel rod was cut and a section was used as sample. It was a radial cut of the pellet included in the cladding (***Figure 2 - a***). The sample was firstly embedded in a low melting point Pb-Bi alloy under vacuum. Then, the surface was mechanically polished with SiC and then with diamond suspensions down to 0.25 µm grade. During the final step, colloidal suspension of silica with a particle size of 0.02 µm was used.

The closed porosity of the sample, determined by immersion in bromobenzene and corrected from the solid swelling of 0.64%/10 GWd/tU [14], is about 3.1%. Every test was conducted in the sample center where the doping rate, and thus the grain size, is constant, with an average size of around 60 µm (***Figure 1***).

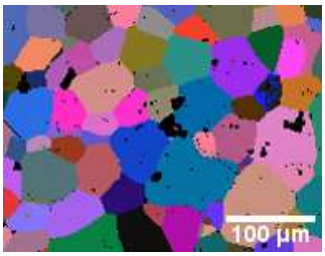

Figure 1: EBSD map of the irradiated UO_2 sample showing its microstructure.

2.2. *Specimen preparation*

The specimens were successfully prepared in the fragmented pellet (***FIGURE 2 - A***), between the macroscopic cracks generated during the irradiation (***FIGURE 2 - B***). A pentagonal section of cantilevers was used as it enables a preparation at any position of the sample surface [15], while square section beams can only be milled on a perpendicular edge of the sample because of FIB angular constraints. Two kinds of specimen were used: notched cantilevers for K_{IC} measurements (***FIGURE 2 – C)*** and un-notched cantilevers for σ_R measurements (***FIGURE 2 – D***). Specimens with typical dimensions of 5x5x17 µm were milled in single grains.

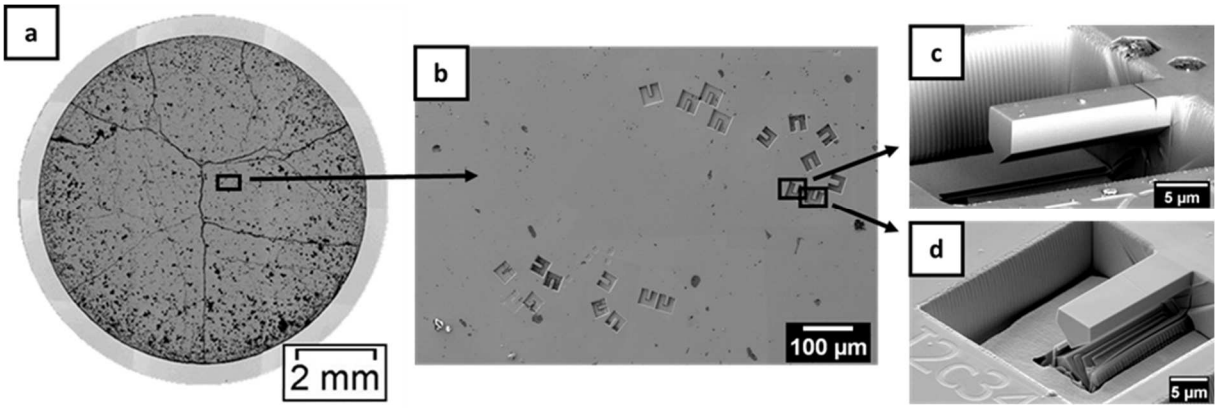

Figure 2: Pictures of a UO_2 fuel irradiated at 34.1 GWd/tU in PWR. (a) Optical macrograph of the sample: a radial cut of a pellet included in the cladding. (b) SEM image of the area framed in black in (a), where a dozen of micro-cantilevers were prepared. (c)(d) SEM image of the area framed in (b), (c) SEM image of a notched specimen and (d) SEM image of an un-notched specimen; both ready to be tested.

Micro-cantilevers were prepared with a Focalized Ion Beam (FIB) of a shielded dual beam microscope Auriga 40 (Carl Zeiss, Oberkochen, Germany), using gallium ions accelerated at 30 kV. At first, every specimen was oriented in order to test specific crystalline fracture planes (perpendicular to the micro-cantilever axis and perpendicular to the sample surface) thanks to Electron BackScatter Diffraction (EBSD) measurements, or on grain boundaries thanks to SEM (Scanning Electron Microscope) pictures. EBSD maps were acquired with a Nordlys camera and Aztec software (Oxford Instruments, Abington-on-Thames, UK), with an accelerating voltage of 20 kV. The coarse shape of cantilevers was obtained with an ionic current of 2 nA, undercuts were made with 2 nA, and every surface was polished with a low current of 80 pA. During notch milling, ion beam was normal to the sample surface with a current of 10 pA in order to have a small notch root radius (estimated between 10 nm and 20 nm by FIB cross-section of a notch (***FIGURE 3***)). When the fabrication steps were finished, every specimen was observed by SEM, using a sample tilt up to 54°, in order to measure each of their dimensions.

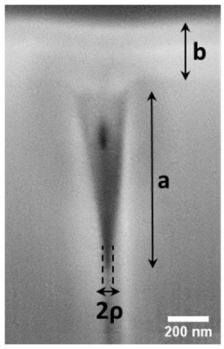

Figure 3 : FIB cross section of a notch prepared on the bulk material with an ionic current of 10 nA. The notch root radius ρ is estimated between 10 nm and 20 nm on this SEM picture. a is the notch depth, and b is the platinum layer deposited to protect the surface during the FIB milling.

Some cantilevers were also prepared to test grain boundaries. Only general high-angle grain boundaries were chosen because of their larger availability. To find a grain boundary perpendicular to the sample surface, a grain boundary between two large grains was chosen. The fuel was then excavated around it by FIB milling in order to visualize its orientation in the sample depth. If its direction was almost perpendicular to the surface, a specimen was prepared, if not, the process was stopped and another grain boundary was selected. Around 25% of excavated grain boundaries had an appropriate orientation and were finally used to mill a micro-cantilever.

2.3. Testing procedure

Every specimen was bended up to fracture, inside the SEM/FIB chamber with a nano-indenter NHT² (CSM Instruments, Peseux, Switzerland), using a force controlled mode at a speed of 0.05 $mN.s^{-1}$. The specimen was pre-tilted in a sample holder at 70° from the SEM stage and the nano-indenter was fixed to the SEM chamber gate with an angle of 20° between the indentation tip and the stage. Finally, the indentation tip direction was normal to the sample surface.

A cube corner tip was used because it allows a good visibility of the sample surface by SEM during the *in situ* loading. To control the loading point position, a very low load of 0.1 mN was firstly applied, which makes a mark on the sample without any risk of cantilever fracture. If the mark was not centered on the cantilever width, the sample was slightly moved and the pre-positioning protocol was repeated. This method allows a very accurate positioning of the loading point.

For every bending test, a SEM video and a load-displacement curve were recorded. This curve exhibits a clear load drop at the failure of the cantilever, allowing a precise measurement of the fracture load. The displacement measured has to be corrected from the penetration of the tip in the material [16]. To do so, an indentation test was made on the bulk material next to each cantilever up to the load corresponding to the fracture load of the specimen. The displacement measured by indentation was then subtracted to the raw displacement of the bending.

3. Methods

3.1. Fracture stress σ_R

Fracture stress was determined from un-notched cantilevers (***FIGURE 2 – D***) using an analytical solution calculated by equation (1), where P_c is the measured fracture load, L the distance between the cantilever fracture plan and the loading point, z is the height between the surface of the beam surface and its gravity center and I_G its moment of inertia, as described in [7].

$$\sigma_R = \frac{P_c . L . z}{I_G} \quad (1)$$

3.2. Fracture toughness K_{IC}

The fracture toughness K_{IC} was determined from tests performed on notched cantilevers (***Figure 2 – c***). As the studied material is brittle, its fracture toughness can be evaluated from linear elastic fracture mechanics. In addition, it has already been seen in the literature that on brittle materials, using a FIB notch as a starter crack with a notch root radius of less than 50 nm gives reliable results for fracture toughness [10]. On macroscopic specimens and on brittle materials, a notch root radius ρ, lower than 10 µm, can be considered sharp enough to estimate the fracture toughness [17]. In [17], the specimens length L was 20 mm, leading to a ρ/L ratio of about $0.5.10^{-3}$. In this work, the notch radius ρ is evaluated at around 10-20 nm (***Figure 3***) for specimens with a length around 20 µm. So, the ratio ρ/L for micro-cantilevers lies between $0.5.10^{-3}$ and 1.10^{-3}, close to the ratio recommended for macroscopic samples.

An analytical solution was used to calculate the K_{IC} of each specimen, using equation (2) and assuming that the notch acts as a perfect crack. In this case, the fracture stress σ_R was calculated using equation (1) considering an un-notched specimen with the same dimensions. a is the notch depth and $\alpha(a/2z)$ is the shape factor [7][18].

$$K_{Ic} = \sigma_R . \sqrt{\pi . a} . \alpha\left(\frac{a}{2z}\right) \quad (2)$$

4. Results

For both notched and un-notched cantilevers, every load-displacement curve was linear up to fracture after correction from the penetration of the tip, confirming the hypothesis of elastic behavior up to fracture (***Figure 4***). Some cyclic tests were also carried out, with loading/unloading cycles. The principle was to apply a load lower than the fracture force, then unload the specimen, and repeat the process while increasing the load at each step until the specimen failed. For each of these tests, a SEM video was recorded and showed in all cases a full elastic recovery of the micro-cantilever after unloading.

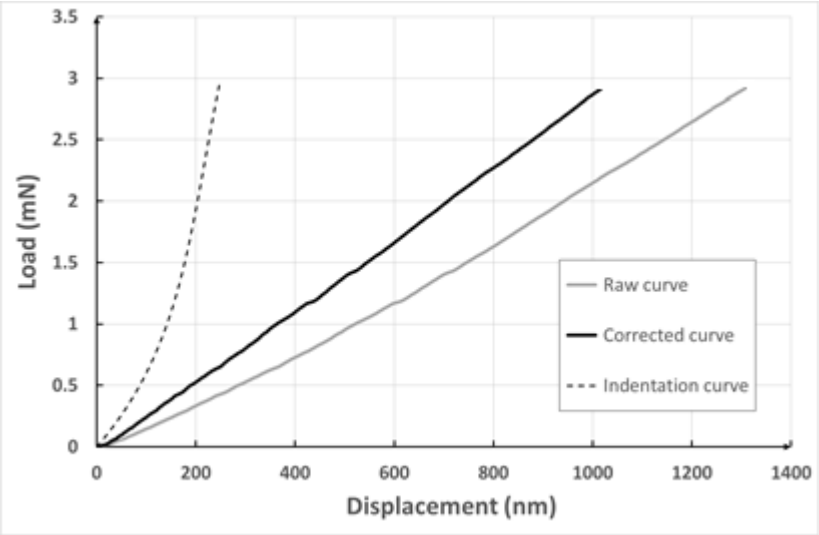

Figure 4 : Typical load-displacement curves of a micro-cantilever bending test. Raw curve: obtained during the bending test. Indentation curve: conducted next to the micro-cantilever specimen up to the fracture load measured on the raw curve. Corrected curve: obtained by subtraction of the indentation displacement from the raw curve displacement.

4.1. Un-notched cantilevers

Nine un-notched cantilevers were tested and each one tested a family of crystalline plane, this plane being perpendicular to the beam axis, and thus to the sample surface. Two were milled in order to test a {100} family plane. Five were prepared to test {110} planes, among them three were in the same grain and thus with exactly the same crystallographic orientation (two of them had no load and displacement recorded because of a technical issue). Two specimens were milled to test {111} planes. Every specimen broke, as expected, at the cantilever base, where the stresses are the highest.

Fracture surface morphology differs considerably with the crystallographic orientation (***FIGURE 5***). For the {100} orientation, fracture surfaces are not smooth and deviate slightly from the targeted plane, normal to the beam axis (***FIGURE 5 - A***). From the stereographic projection of the tested grain, the observed deviation does not seem to be toward a specific family plane. Concerning {110} orientation, fracture planes are smooth but deviate considerably from the targeted plane (***FIGURE 5 - B***). Four times out of five tested specimens, fracture surfaces were split into two different surfaces, each being not normal to the beam axis. The angle between these two surfaces is very close to the angle between two {111} planes measured on the stereographic projection. The three specimens prepared in a same grain showed a very reproducible fracture behavior with a fracture surface made of two planes separated by an angle between 125° and 130°, against 123° between the two closest {111} planes measured on the stereographic projection. These observations indicate that the fracture deviations to {111} planes are reproducible for a same grain. Finally, specimens testing {111} planes broke with a smooth fracture surface, normal to the cantilever axis (***FIGURE 5 - C***).

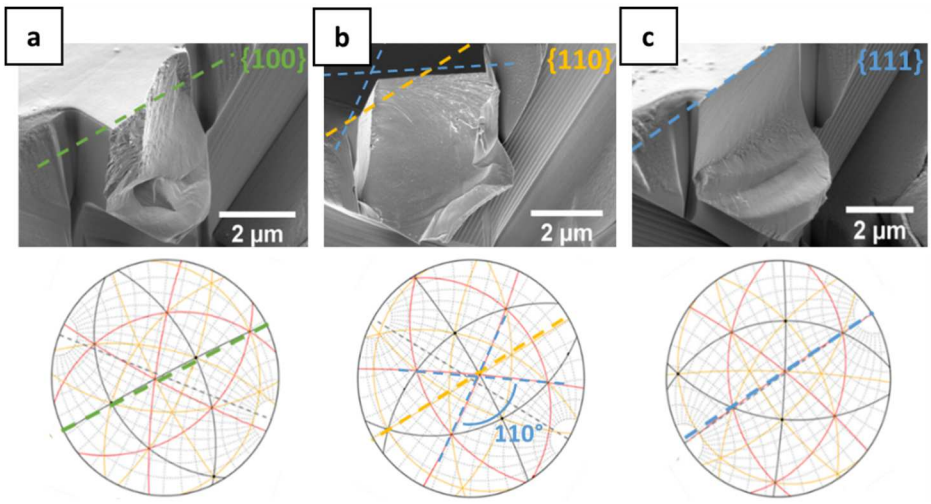

Figure 5 : SEM images of fracture surfaces of different un-notched micro-cantilevers testing three various families of plane: (a): {100}, (b): {110} and (c): {111}. Dotted lines represent the trace of crystallographic planes on the sample surface: green represents {100}, yellow {110} and blue {111}. Stereographic projection of crystalline planes associated to the tested grains are given bellow, where black lines represent {100} planes, yellow lines {110} and red lines {111}.

Three un-notched cantilevers were also prepared to test grain boundaries. Grain boundaries were not located at the specimen base in order to be visible by SEM on the cantilever sides (***FIGURE 6 - A***). Every specimen broke along the grain boundary, and the fracture surfaces followed exactly the grain boundary, even if the stresses are higher at the base of the cantilever. Moreover, the fracture surface appears as very different from intra-granular tests and exhibits irradiation defects: bubbles and precipitates of fission products (***FIGURE 6 - B***).

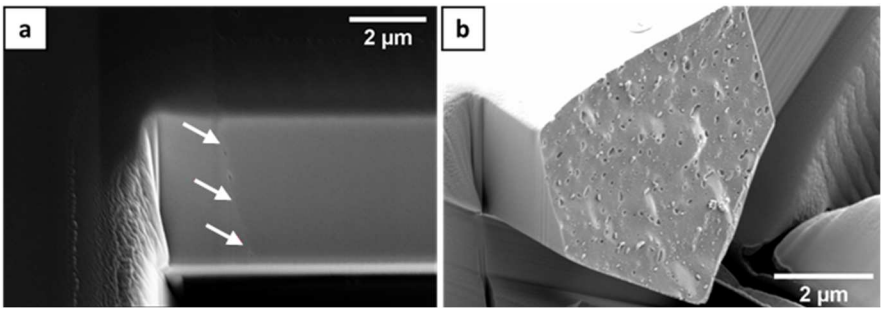

Figure 6 : SEM images of an un-notched cantilever testing a grain boundary: (a) before fracture, showing a side of the cantilever where the grain boundary is visible and pointed with white arrows; (b) after fracture, showing a fracture surface covered by irradiation defects : fission products gas bubbles (dark points) and fission products precipitates (bright points).

The fracture stress σ_R for each tested microstructural feature are reported in ***TABLE 1***. Fracture strength of {100}, {110} and {111} planes in single grains lies in the range of: 3.30 – 3.90 GPa, 2.43 – 2.62 GPa and 1.95 – 2.55 GPa respectively, while it ranges between 0.74 GPa and 1.60 GPa on grain boundaries.

Table 1 : Fracture stress σ_R (GPa) of each tested microstructural feature: {100}, {110}, {111} planes and grain boundaries (GB).

Tested feature	*Fracture stress σ_R (GPa)*			
	Sample number			**Average**
	1	2	3	
{100}	3.30	3.90	-	3.60
{110}	2.43	2.55	2.62	2.53
{111}	1.95	2.55	-	2.25
GB	0.74	1.46	1.60	1.27

4.2. Notched cantilevers

Nine notched cantilevers were prepared in order to test specific crystallographic fracture planes: three into {100} planes, two into {110} planes and four into {111} planes. Every specimen broke at the notch location, and the fracture surface followed the plane defined by the notch (***FIGURE 7***).

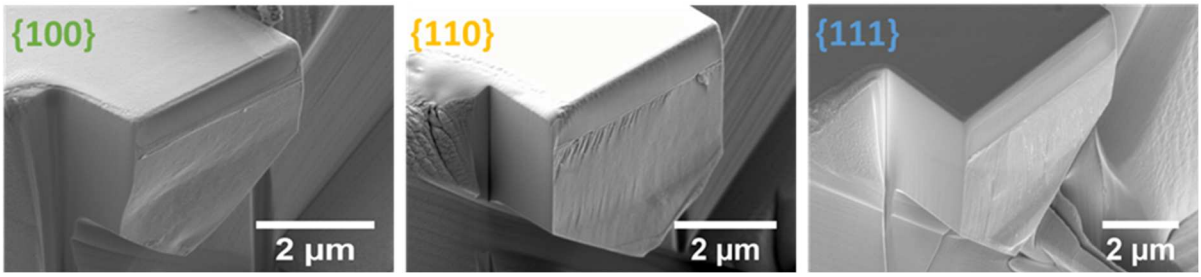

Figure 7 : SEM images of fracture surfaces of different notched micro-cantilevers testing three various families of plane: {100}, {110} and {111}.

Fracture toughness values for each tested plane are reported in (***TABLE 2***). The fracture toughness of {100} planes is in the range of 1.51 - 1.69 MPa.m$^{0.5}$, {110} planes in the range of 1.72 - 1.89 MPa.m$^{0.5}$ and {111} planes in the range of 1.24 - 1.62 MPa.m$^{0.5}$.

Table 2 : Fracture toughness K_{IC} of each tested family of planes {100}, {110} and {111}.

Tested plan	*Fracture toughness K_{IC} (MPa.m$^{0.5}$)*				
	Sample number				**Average**
	1	2	3	4	
{100}	1.51	1.65	1.69	-	1.62
{110}	1.72	1.89	-	-	1.80
{111}	1.24	1.28	1.32	1.62	1.37

Three notched specimens were also milled on a grain boundary. In each case, during the final step of the milling process, the cantilever exhibited an irreversible deformation: it deforms upward, leading to an opening of the grain boundary from the bottom of the specimen. Every notched micro-cantilever prepared on a grain boundary showed a crack along this grain boundary and created during the milling (***FIGURE 8 - A***). Fracture tests were still conducted, leading to a very low fracture stress, around 0.1 mN. The fracture surface in such a case is very similar to the one observed by fracture of an un-notched cantilever prepared on a grain boundary showing irradiation defects (***FIGURE 8 - B***), confirming that the crack generated during the milling process follows the grain boundary.

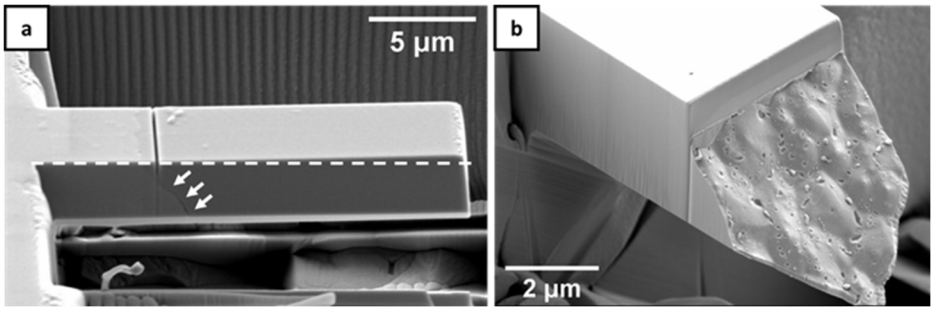

Figure 8 : SEM images of a notched cantilever prepared to test a grain boundary: (a) the cantilever before the bending test presents an irreversible deformation upward showed by the white dotted line, which induced a crack on the grain boundary, pointed by white arrows; (b) after fracture, the fracture surface shows many irradiation defects (bubbles and precipitates of fission products).

5. Discussion

5.1. Comparison with literature data

In the literature, fracture properties are only available on the fresh UO_2 fuel.

The fracture toughness measured on macroscopic fresh UO_2 samples by Evans *et al.* [5] by SENB (Single Edge Notched Beam) lies between 1.4 ± 0.15 MPa.m$^{0.5}$ and 1.8 ± 0.2 MPa.m$^{0.5}$. Fracture toughness results of the present work obtained by a micro-cantilever method inside single grains of an irradiated UO_2 are in good agreement with [5], with an average value around 1.5 MPa.m$^{0.5}$ (***TABLE 2***). These measurements are not immediately comparable since one was made on the fresh fuel at the macroscopic scale and the other on an irradiated fuel at the microscopic scale. But still, they are close and thus the fracture toughness presumably does not suffer from an extensive scale effect.

Frazer *et al.* [12] measured fracture stresses of fresh UO_2 single crystal with micro-cantilever bending tests and found values around 3.3 GPa. In the present work, the fracture stress of irradiated fuel is in average around 2.7 GPa in grains and around 1 GPa on grain boundaries (***TABLE 1***). It shows that irradiation only seems to have a limited influence on the fracture stress measured in grains, but leads to a weakening of grain boundaries. These micro-mechanical values are much higher than the fracture stress of fresh UO_2 measured at the macroscopic scale, around 100-200 MPa [5][19][20]. This observed scale effect on the fracture stress is likely partly due to a lower probability to find a large defect inducing the failure in small specimens (statistical size effect). In microscopic samples, porosities and other flaws have a few micrometers size, or even less, while biggest defects of macroscopic samples have a size of several tens of micrometers. The effect of flaws on the measured fracture stress is more discussed in another related study [21].

5.2. Grain boundaries testing

Grain boundaries exhibit a significant lower fracture stress than grains, for any crystallographic orientation (***TABLE 1***). It is probably due to a lower resistance of the grain boundaries and/or to the presence of defects segregated on grain boundaries, such as bubbles and precipitates of fission products. These defects are small and have a diameter under 100 nm as measured by SEM (***FIGURE 6***). However, they induced a reduction of the apparent fracture stress by about a factor 2 compared to grain values. In single grains, at the magnification used, there is no visible irradiation defect on fracture surfaces (***FIGURE 5***). This decreased resistance in the presence of defects is in good agreement with the observations of Frazer *et al.* [12], who have shown by a micro-cantilever method applied on fresh UO_2 that the fracture stress of a specimen with porosities (diameter of around 1 µm) has a fracture stress between 5 and 10 times lower than a specimen milled into a dense single

crystal. It is also consistent with the apparent weakness of grain boundaries observed by indentation testing (***FIGURE 9***).

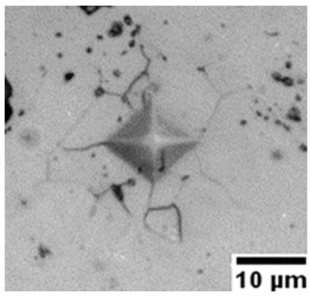

Figure 9 : Optical micrograph of a Vickers indentation imprint and cracks generated by it, on a nuclear fuel sample irradiated at 16 GWd/tU. The path of cracks is strongly influenced by grain boundaries (CEA, unpublished work).

The preparation of notched cantilevers for grain boundary testing was not successful. The irreversible deformation of cantilevers appearing during the fabrication process is potentially induced by residual stress release. This has only been noted on notched cantilevers milled in irradiated fuel and including a grain boundary and was not observed neither on notched or un-notched cantilevers milled in a single grain of cubic zirconia [7] nor in single grain or grain boundary of fresh UO_2 fuel [21]. In irradiated fuel, no deformation was visible either for notched specimens milled into a single grain or for un-notched specimens milled around a grain boundary. Thus, the combination of the notch milling with the presence of a grain boundary seems to lead to an irreversible deformation during the fabrication process of cantilevers on the irradiated fuel. It could be induced by the release of residual stresses by the FIB milling, and the residual stress field is potentially present because of irradiation and/or because of pressurized bubbles formed at grain boundaries [22]. Milling a notch reduces the effective section of the cantilever and thus its stiffness, and probably changes the residual stress state around the notch [23] in the proximity of the grain boundary, which can finally lead to an irreversible deformation and to the fracture of the specimen before testing.

5.3. Influence of crystallography

Fracture surfaces of un-notched cantilevers (***FIGURE 5***) seem to indicate that the fracture is easier along a {111} plane than along the other tested planes. Indeed, fracture surfaces of {111} orientation are smooth and normal to the beam axis, whereas fracture surfaces aiming {100} and {110} deviate from the targeted plane. Fracture stress measured on un-notched cantilevers (***TABLE 1***) indicates that {100} planes appears as more resistant than {110} and {111} planes, and these two last families of plane are difficult to differentiate in terms of fracture stress. However, fracture surfaces of {110} oriented specimens deviate toward {111} planes, indicating a lower resistance of {111} compared to {110} planes. The close values of fracture stresses for these two families of planes may eventually be explained by the fact that for {110} orientation, the fracture deviates toward {111} planes. Finally, the analysis of both fracture surfaces and fracture stresses of un-notched cantilevers gives the following orders of resistance: {100} < {111} and {110} < {111}. Unlike the {110} orientated specimens, {100} orientated ones do not exhibit a deviation of fracture surface toward {111} planes. As in a cubic crystal {111} planes are angularly closer to a {110} plane than any {100} plane, it is not possible to conclude here on any order of resistance between {100} and {110}.

For notched specimens, fracture surfaces (***FIGURE 7***) are similar between the different tested crystallographic orientations. Fracture toughness (***TABLE 2***) are close between the different planes, even if {111} seems to have a slightly lower fracture toughness, {100} is intermediate and {110} has a slightly higher fracture toughness. This order was already noticed for fracture toughness measurements on cubic zirconia [7].

Then, {111} seems to be, on both notched an un-notched specimens, the most favorable type of plane for fracture. In another hand, for a fluorite structure such as uranium dioxide, cleavage is expected to be on {111} plane [24]. Moreover, the order of both fracture stress and fracture toughness expected by different simulations in a UO_2 crystal is {111} < {110} < {100} [25][26]. Whereas the lower value for {111} is confirmed in this work, the unexpected order of resistance of toughness for {110} and {100} planes may be explained by a possible influence of the FIB milling process of the notch [23] on the fracture toughness determination. It could be, for example, due to ion implantation, already known to influence the toughness measurement as noted on some materials [27] but not on others [15]. It is likely that ion milling could be influenced by the crystallographic orientation of the tested grain, whether in terms of ion implantation or of shape or sharpness of the notch."

Conclusion

This work shows the feasibility of micro-bending tests to assess the fracture properties of the irradiated PWR fuel, despite the important constraints linked to the testing of such irradiated material. This work leads to the following observations:

- For the first time, the fracture parameters of the irradiated UO_2 fuel have been evaluated by a bending method. The fracture stresses measured ranges between 1.95 GPa and 3.90 GPa for single grains, and between 0.74 GPa and 1.60 GPa for grain boundaries. Fracture toughness has also been measured thanks to notched cantilevers, ranging between 1.24 $MPa.m^{0.5}$ and 1.89 $MPa.m^{0.5}$ in single grains.
- Testing specimens milled along different orientations inside grains shows a clear dependence of the fuel fracture properties with the crystallography. For both un-notched and notched specimens, {111} planes appear to be weaker than the other planes, which is expected on UO_2 crystals. However, for {100} and {110} planes, the difference of fracture behavior is less clear.
- Micro-bending tests appear as very attractive to test interfaces, such as grain boundaries of the fuel. Only their fracture stresses have been evaluated in this work, because for notched cantilevers, it seems that residual stresses induce irreversible deformations and cracks in the specimens during the milling process. However, the comparison of fracture stress between grains and grain boundaries shows a weakening of the grain boundaries with the irradiation, probably induced by the formation of irradiation defects such as fission gas bubbles and fission precipitates.

All these information are valuable to improve the general understanding of the nuclear fuel fracture properties but also to improve numerical modelling of its behavior under irradiation, including accidental scenarios for which it is important to characterize the strength of grain boundaries.

Acknowledgements

This research project was mainly funded by CEA and INSA-Lyon, and was also financially supported by EDF and Framatome. The authors are grateful to Jean Noirot for his improvements of the manuscript.

References

[1] C. Nonon *et al.*, "Impact of fuel microstructure on PCI behaviour," *Proc. a Tech. Comm. Meet. IAEA*, 2003.

[2] D. Lespiaux, J. Noirot, and P. Menut, "Post-test examinations of high burnup PWR fuels submitted to RIA transients in the CABRI facility," *Proc. Int. Top. Meet. LWR fuel Perform.*,

1997.

[3] Nuclear Energy Agency, “Report on fuel fragmentation relocation and dispersal,” 2016.

[4] B. Michel, J. Sercombe, G. Thouvenin, and R. Chatelet, “3D fuel cracking modelling in pellet cladding mechanical interaction,” *Eng. Fract. Mech.*, vol. 75, no. 11, pp. 3581–3598, 2008, doi: 10.1016/j.engfracmech.2006.12.014.

[5] A. G. Evans and R. W. Davidge, “The strenght and fracture of stoichoimetric polycristalline UO2,” *J. Nucl. Mater.*, vol. 33, no. 33, pp. 249–260, 1969.

[6] R. F. Canon, J. T. A. Roberts, and R. J. Beals, “Deformation of UO2 at high temperatures,” *J. Am. Ceram. Soc.*, vol. 54, no. 2, pp. 105–112, 1971, doi: 10.1111/j.1151-2916.1971.tb12230.x.

[7] R. Henry *et al.*, “Local fracture toughness measurements in polycrystalline cubic zirconia using micro-cantilever bending tests,” *Mech. Mater.*, vol. 136, 2019.

[8] C. E. Athanasiou *et al.*, “High toughness carbon-nanotube-reinforced ceramics via ion-beam engineering of interfaces,” *Carbon N. Y.*, vol. 163, pp. 169–177, 2020, doi: 10.1016/j.carbon.2020.02.075.

[9] V. Pejchal, M. Fornabaio, G. Žagar, and A. Mortensen, “The local strength of individual alumina particles,” *J. Mech. Phys. Solids*, 2017, doi: 10.1016/j.jmps.2017.08.005.

[10] G. Dehm, B. N. Jaya, R. Raghavan, and C. Kirchlechner, “Overview on micro- and nanomechanical testing: New insights in interface plasticity and fracture at small length scales,” *Acta Mater.*, 2017, doi: 10.1016/j.actamat.2017.06.019.

[11] R. Pippan, S. Wurster, and D. Kiener, “Fracture mechanics of micro samples: Fundamental considerations,” *Mater. Des.*, vol. 159, pp. 252–267, 2018, doi: 10.1016/j.matdes.2018.09.004.

[12] D. Frazer, “Elevated temperature small scale mechanical testing of uranium dioxide,” phD thesis, Berkeley University, 2018.

[13] P. Hosemann, C. Shin, and D. Kiener, “Small scale mechanical testing of irradiated materials,” *J. Mater. Res.*, vol. 30, no. 09, pp. 1231–1245, 2015, doi: 10.1557/jmr.2015.26.

[14] J. Noirot *et al.*, “High burnup changes in UO2 fuels irradiated up to 83 GWd/t in M5® claddings,” *Nucl. Eng. Technol.*, vol. 41, no. 2, pp. 155–162, 2009, doi: 10.5516/NET.2009.41.2.155.

[15] B. N. Jaya, C. Kirchlechner, and G. Dehm, “Can microscale fracture tests provide reliable fracture toughness values ? A case study in silicon,” *J. Mater. Res.*, vol. 30, no. 5, 2015.

[16] E. Camposilvan, O. Torrents, and M. Anglada, “Small-scale mechanical behavior of zirconia,” *Acta Mater.*, vol. 80, pp. 239–249, 2014, doi: 10.1016/j.actamat.2014.07.053.

[17] T. Nishida, T. Hanaki, and G. Pezzotti, “Effect of root notch radius on the fracture toughness of a fine-grained alumina,” *J. Am. Ceram. Soc.*, vol. 77, no. 2, pp. 606–608, 1994.

[18] H. Chan, S. G. Roberts, and J. Gong, “Micro-scale fracture experiments on zirconium hydrides and phase boundaries,” *J. Nucl. Mater.*, vol. 475, pp. 105–112, 2016, doi: 10.1016/j.jnucmat.2016.03.026.

[19] J. M. Gatt, J. Sercombe, I. Aubrun, and J. C. Ménard, “Experimental and numerical study of fracture mechanisms in UO2 nuclear fuel,” *Eng. Fail. Anal.*, vol. 47, pp. 299–311, 2015, doi: 10.1016/j.engfailanal.2014.07.019.

[20] K. C. Radford, “Effect of fabrication parameters and microstructure on the mechanical strenght of UO2 fuel pellets,” *J. Nucl. Mater.*, vol. 84, pp. 222–236, 1979.

[21] R. Henry *et al.*, “Irradiation effects on the fracture properties of UO2 fuels studied by micro-mechanical testing,” *Submitt. to J. Nucl. Mater.*, 2020.

[22] C. Cagna, “Influence des gaz de fission sur l’état mécanique des combustibles oxydes irradiés,” phD thesis, ENSAM Paris, 2016.

[23] A. D. Norton, S. Falco, N. Young, J. Severs, and R. I. Todd, “Microcantilever investigation of fracture toughness and subcritical crack growth on the scale of the microstructure in Al2O3,” *J. Eur. Ceram. Soc.*, vol. 35, no. 16, pp. 4521–4533, 2015, doi: 10.1016/j.jeurceramsoc.2015.08.023.

[24] R. G. Robins and P. J. Baldock, “Uranium oxide Cleavage,” *J. Am. Ceram. Soc.*, vol. 43, no. 4, p. 228, 1960.

[25] L. Li, W. Bao-Tian, and Z. Ping, “Ideal strengths and bonding properties of UO2 under tension,” *Chinese Phys. Lett.*, vol. 32, no. 3, 2015, doi: 10.1088/0256-307X/32/3/037102.

[26] G. Sattonnay and R. Tétot, “Bulk, surface and point defect properties in UO2 from a tight-binding variable-charge model,” *J. Phys. Condens. Matter*, vol. 25, 2013, doi: 10.1088/0953-8984/25/12/125403.

[27] J. P. Best *et al.*, “A comparison of three different notching ions for small-scale fracture toughness measurement,” *Scr. Mater.*, vol. 112, pp. 71–74, 2016, doi: 10.1016/j.scriptamat.2015.09.014.